CNRS	NIKHEF	INFN
Centre National de la Recherche Scientifique	*Nationaal instituut voor subatomaire fysica*	*Instituto Nazionale di Fisica Nucleare*

Advanced Virgo Output Mode Cleaner: refinement of the design and polishing specifications

P.A. Casula, L. Digallo, R. Gouaty, F. Marion, B. Mours, L. Rolland

VIR-0319A-12

September 13, 2012

Contents

1 Introduction

Preliminary specifications of the output mode cleaner (OMC) cavity for Advanced Virgo have been discussed in previous notes [1, 2] and a baseline design made of two OMC cavities in series has been described in [3]. Since then, additional checks for the polishing specifications have been made [4, 5]. The goal of this document is to present the refined design of the Advanced Virgo OMC cavities. A slight modification with respect to the design presented in [3] is introduced: the proposal is to have a single spherical surface per OMC cavity instead of two.

Section 2 gives the motivations for having one spherical surface per OMC cavity. The choice of the nominal radius of curvature is explained in section 3. The refined OMC design is presented in section 4. The filtering performances that are expected with this design are given in section 5. Section 6 gives the polishing specifications that will be provided to the selected polishing company. Finally section 7 presents the OMC loss budget that can be expected according to all these specifications.

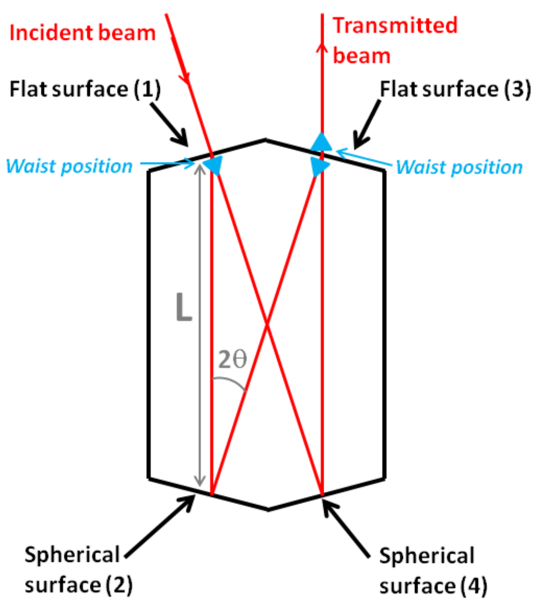

(a) TDR design

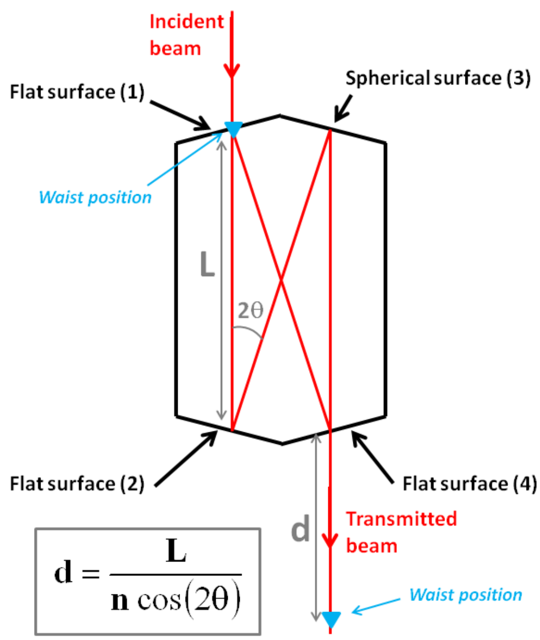

(b) Refined design

Figure 1: Schematic drawing of the OMC cavity. Left side: configuration with two spherical surfaces. Right side: configuration with one spherical surface. Small blue triangles indicate the waist positions.

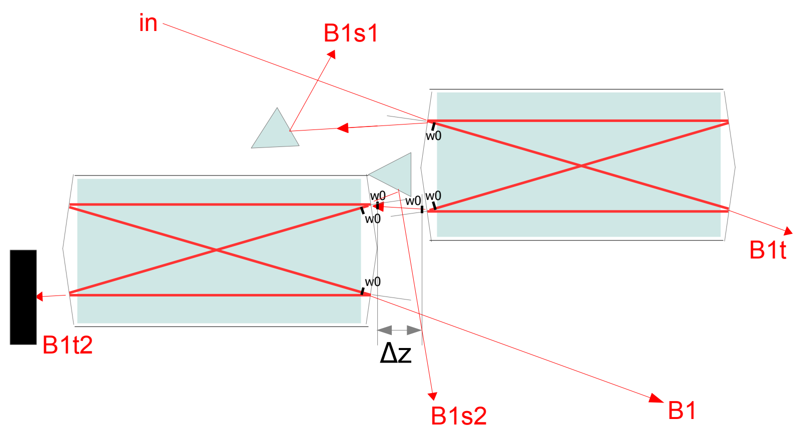

Figure 2: Optical layout obtained with two spherical surfaces per OMC cavity (TDR baseline).

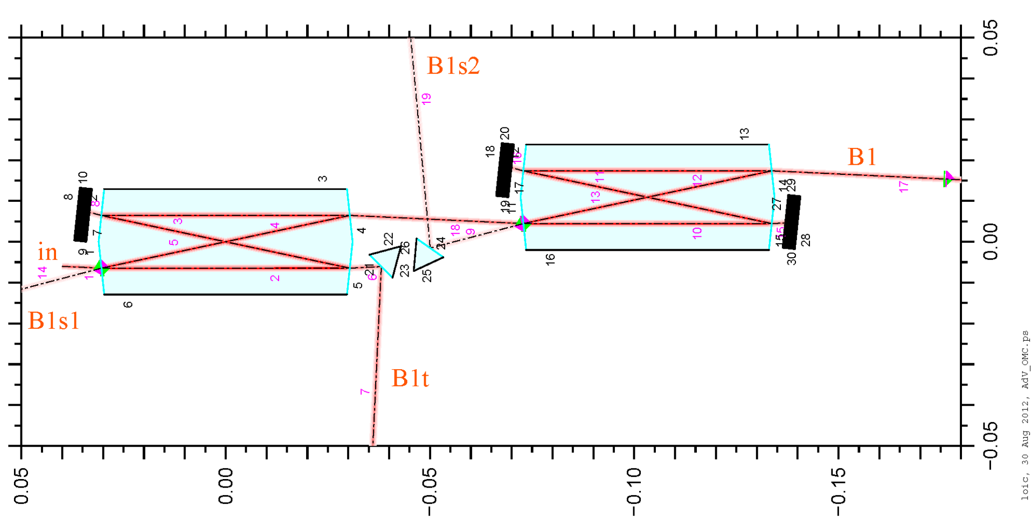

Figure 3: New optical layout of the mode cleaner cavities, with one spherical surface per cavity. This drawing has been obtained with the Optocad simulation. It should be noticed that the small prisms used to extract the B1t abd B1s2 beams are only drawn by way of example. The beam extraction might be performed in a different way.

2 Motivations for a single spherical surface

In the baseline design presented in [3], each OMC cavity is made of two flat surfaces and two spherical surfaces, as it is schematized in Fig. 1a. With this configuration the waist position of the transmitted beam is located in the vicinity of the flat surface #3 (using the surface numbering convention shown in Fig. 1). Given L the lengh of the cavity as measured along the beam optical path between surfaces #1 and #2, and θ the inclination angle of each surface, the distance between the waist of the transmitted beam and surface #3 is given by:

$$d = \frac{L}{2n}\left(\frac{1}{cos(2\theta)} - 1\right) \tag{1}$$

where n is the refraction index of fused silica (n=1.44963).
With $L = 60\ mm$ and $\theta = 8.876°$ (parameters found in Fig. 7.4 of the TDR), one obtains: $d \approx 1\ mm$.

In order to minimize the risk of misalignments between the two OMC cavities, a solution without any intermediate optics along the path between the two cavities is strongly favoured. In order to obtain a perfect matching between the two OMC cavities, the second OMC should then be placed at a distance corresponding to $2d \approx 2\ mm$. This is not possible because of the need to extract the beam reflected by the second OMC (called $B1s2$ in Fig. 2). Thus the solution presented in the TDR [3] resulted from a trade-off between the necessity to extract the $B1s2$ beam and the goal of keeping the two OMC cavities as close as possible to each other to maximize the beam matching. The optical layout that was proposed in the TDR is shown in Fig. 2. In this layout the theoretical waits of the two cavities are separated by a distance under vacuum $\Delta z \approx 9\ mm$, which induces mismatching losses of the order of 0.1%. Although the amount of losses is acceptable, this layout can be challenging for the mechanical design due to its extreme compactness. Therefore a refinement of the design is proposed as explained below.

In the refined design, the OMC cavity is made of three flat surfaces and only one spherical surface, as schematized in Fig. 1b. With this configuration the ideal waist of the input beam is located exactly on the surface #1, and the waist of the transmitted beam is separated from the surface #4 by the distance:

$$d = \frac{L}{ncos(2\theta)} \tag{2}$$

With $L = 60.82\ mm$ and $\theta = 6°$ (parameters found in Tab. 1), one obtains $d \approx 42.9\ mm$.
With this new configuration an exact matching of the waists can be fulfilled by placing the second OMC cavity at 42.9 mm from the first cavity. This solution is thus better for minimizing losses. More importantly this configuration eases the extraction of the B1s2 beam and relaxes the requirement on compactness for the mechanical design. The new optical layout has been checked with the Optocad simulation and is presented in Fig. 3. This layout is now considered as the reference design in the following.

3 Selection of the radius of curvature

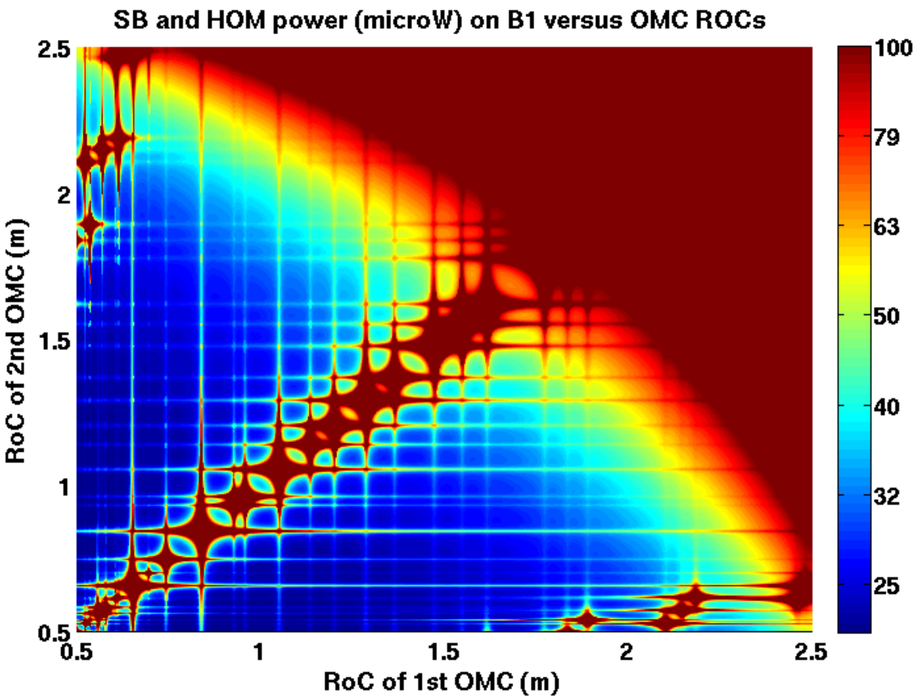

Figure 4: Sum of side bands and high order modes in transmission of the OMC (B1 beam) as a function of the two OMC RoCs. The color scale is given in μW and has been bounded to $100\mu W$ for clarity reasons.

The change in the baseline design discussed in section 2 requires an adjustement of the surface radius of curvature (RoC). Moreover, in May 2012 it has been suggested by the STAC to investigate the possible benefits of using different RoCs for the two cavities. The conclusion of this investigation is presented in this section.

Aside the change concerning the number of spherical surfaces and the value of the RoC, the other OMC parameters (finesse F_{OMC}, geometrical length L_{geo}, and optical length L_{opt}) are kept unchanged with respect to [3]. Their values are provided in Tab.1. The geometrical length and the optical length are related to the parameters L and θ used in Section 2 as follows:

$$L_{geo} = \frac{L}{2}\left(1 + \frac{1}{cos(2\theta)}\right) \tag{3}$$

$$L_{opt} = 2nL_{geo} \tag{4}$$

The value of the waist w_0 is related to the radius of curvature of the spherical surface (ρ)

according to the relation:

$$w_0 = \sqrt{\frac{\lambda}{n\pi}\sqrt{2L_{geo}(\rho - 2L_{geo})}} \tag{5}$$

As explained in [3] the choice of the RoC is made according to two criteria:

- The waist of the OMC cavity should not be too small in order to not worsen the amount of back-scattered light that is known to vary as the inverse of the squared waist [6, 7]. Therefore values of the RoC below 500 mm, which correspond to a waist lower than $225\mu m$, are not considered.

- The RoC must be chosen in order to minimize the transmission of the high order modes (HOM) for the carrier and for the side bands at 6.27 MHz and 56.44 MHz. More details are given below.

When the TEM_{00} of the carrier field is kept resonant in the OMC cavity, the OMC transmission of a high order mode (HOM) is given by:

$$T^N_{car} = \frac{1}{1 + \left(\frac{2F_{OMC}}{\pi}\right)^2 sin^2\left(N \times acos\left(\sqrt{1 - \frac{2L_{geo}}{\rho}}\right)\right)} \tag{6}$$

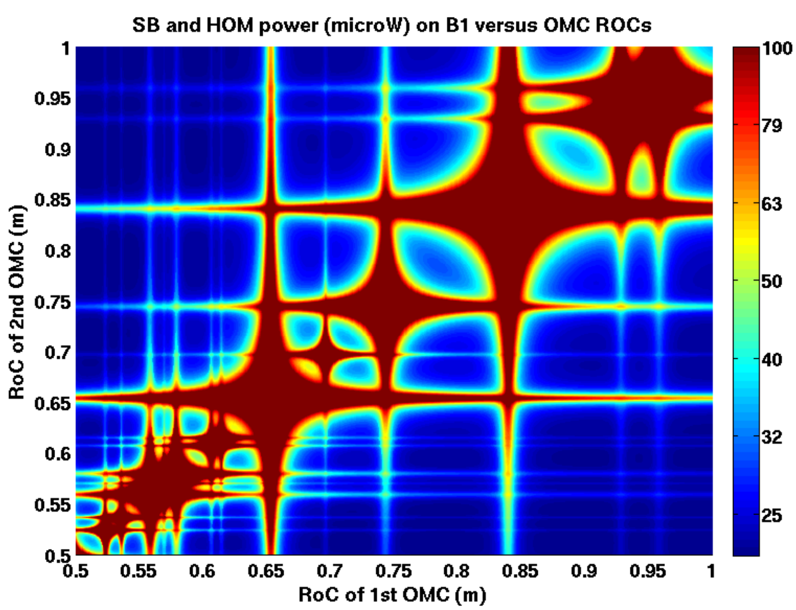

Figure 5: ZOOM: Sum of side bands and high order modes in transmission of the OMC (B1 beam) as a function of the two OMC RoCs. The color scale is given in μW and has been bounded to $100\mu W$ for clarity reasons.

where N stands for the mode order ($N = m + n$, in the case of a $TEM_{m,n}$).
In the case of a left side band (SB) HOM at a modulation frequency f_{mod}, the OMC transmission is given by:

$$T^N_{lsb} = \frac{1}{1 + \left(\frac{2F_{OMC}}{\pi}\right)^2 sin^2\left(-\frac{2\pi f_{mod} l_{opt}}{c} - N \times acos\left(\sqrt{1 - \frac{2L_{geo}}{\rho}}\right)\right)} \tag{7}$$

And for the right side band HOM:

$$T^N_{rsb} = \frac{1}{1 + \left(\frac{2F_{OMC}}{\pi}\right)^2 sin^2\left(\frac{2\pi f_{mod} l_{opt}}{c} - N \times acos\left(\sqrt{1 - \frac{2L_{geo}}{\rho}}\right)\right)} \tag{8}$$

One can define a factor of merit quantifying the expected amount of carrier HOM power transmitted by the two OMCs. This factor of merit is given by:

$$FoM_{car} = \sum_{N=1}^{N=14} T^N_{car,1} T^N_{car,2} P^N_{car} \tag{9}$$

where P^N_{car} stands for the power in the modes of order N before the OMC, $T^N_{car,1}$ and $T^N_{car,2}$ are the transmission factors of the first and second OMC cavities, respectively. These transmission factors are calculated according to equation 6. Only the modes with order $N \leq 14$ are taken into account in the calculation of the FoM, because higher order modes will not be accepted by the system aperture due to their extended spatial profile.
Similarly one can define a factor of merit quantifying the residual side band power (including the fundamental mode and the HOM) after the two OMC cavities as:

$$FoM_{sb} = \sum_{N=0}^{N=14} \frac{1}{2}(T^N_{lsb,1} T^N_{lsb,2} P^N_{sb} + T^N_{rsb,1} T^N_{rsb,2} P^N_{sb}) \tag{10}$$

Finally a combined factor of merit can be defined as:

$$FoM = FoM_{car} + FoM_{sb1} + FoM_{sb2} \tag{11}$$

This factor of merit corresponds to the sum of all high order modes and all side bands components (including the SB TEM_{OO}) that are expected in transmission of the second OMC cavity. The OMC RoCs must be chosen to minimize this factor of merit. The quantity FoM has been evaluated by using the same assumptions on the HOM and SB power before the OMC (values of P^N_{car} and P^N_{sb}) as it has been done in [3] (see Tab. 7.3 and Tab. 7.4 in the TDR).

The factor of merit is plotted as a function of the two OMC RoCs in Fig. 4 for RoC values ranging from 500 mm to 2500 mm, assuming the Advanced Virgo Signal Recycling 125W configuration. A zoom of the same plot for RoC values ranging from 500 mm to 1000 mm is shown in Fig. 5. The color scale representing the amount of power in the HOM and SB components after the second OMC cavity has been bounded to $100\mu W$ for clarity reasons. The specifications on the OMC filtering (provided by ISC in [3]) correspond to $80\mu W$ per side band. Therefore any working point corresponding to a color other than red in Fig. 4 would satisfy the requirements.

Equal RoCs versus unequal RoCs

The only configuration that allows a perfect matching between the two OMC cavities without any intermediate optics is obtained by selecting equal RoCs for the two cavities. This corresponds to the diagonal of the plots shown in Fig. 4 and Fig. 5. With this additional constraint the optimal working point (that minimizes the factor of merit while allowing some error bars of $\approx\ \pm 2$ % on the RoCs) is found near RoC values equal to 800 mm. In this region the local minimum of the factor merit is $30\mu W$, which is well below the requirements ($80\mu W$ per side band).

The previous number can be compared to the absolute minimum of the factor of merit in Fig. 4, which corresponds to $23\mu W$. This means that if we did not impose the constraint of having equal RoCs, we would not gain more than 20% on the filtering performances. In order to keep mismatching losses $\leq$ 0.1% the difference between the two cavity waists must be lower than 3%, which corresponds to an absolute RoC difference of about 80 mm in the region near $\rho = 800\ mm$. With this constraint there is no benefit in selecting two different RoCs.

To conclude, potential benefits of selecting two different RoCs are very marginal and the solution based on two OMC cavities of equal RoCs is preferred because of two advantages:

- it allows a perfect matching between the two cavities without the need for intermediate lenses;
- it gives more flexibility for the use of spare cavities (which reduces the technical risk), and simplify the polishing order (with a potential cost savings).

Based on this study it has been decided that the design should remain based on two identical OMC cavities.

RoC fine tuning

Figure 6 shows the variation of the factors of merit as a function of the OMC RoC, assuming that the RoC of the two cavities are identical, for a geometrical length $L_{geo} = 61.5\ mm$. The total FoM (sum of carrier HOMs, side bands TEM_{00} and HOMs) is minimized for a RoC equal to 783 mm. For this value the estimated contributions of the carrier and the 56.44 MHz side band are equal. One can notice that the $6.27 MHz$ side band does not play any role in the fine

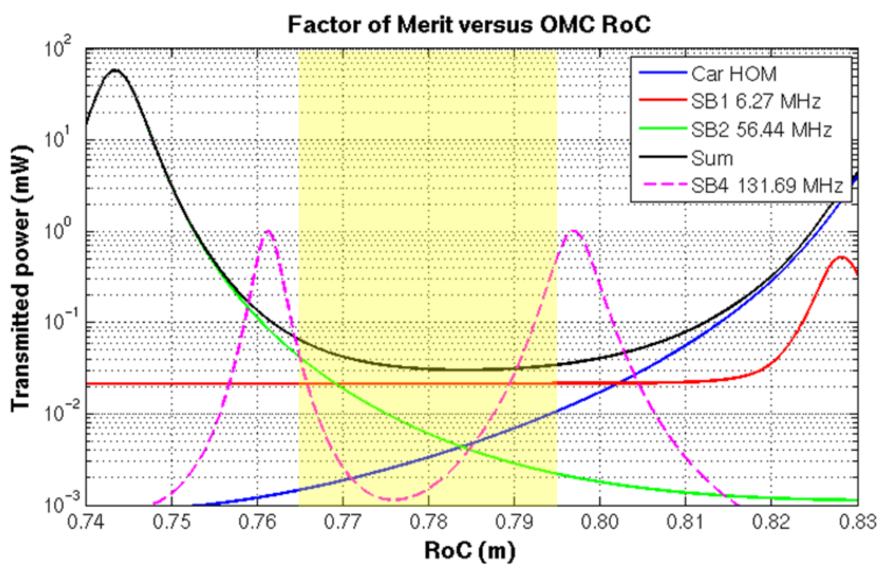

Figure 6: Sum of side bands and high order modes in transmission of the OMC (B1 beam) as a function of the OMC RoC (the two cavities are now considered as identical). The black curve stands for the total factor of merit (FoM) that includes the sum of all carrier high order modes, and all 6.27 MHz and 56.44 MHz side band components. The blue curve corresponds to the carrier FoM (sum of carrier HOMs). The red curve (respectively green) stands for the contribution of the 6.27 MHz (respectively 56.44 MHz) side band. A FoM has also been calculated for the 131 MHz side band and is shown as the purple dotted curve. The yellow shadowed area represents the possible location of the RoC, assuming a nominal value of 780 mm with an allowed error bar of ± 15 mm.

selection of the RoC because its FoM is dominated by the TEM_{00} mode.
An estimation of the FoM for the 131 MHz side band is also shown in Fig. 6 (purple dotted curve). For this side band the modulation index is assumed to be 10 times lower than it is for the other side bands: m = 0.01 (some uncertainty remains on this value as the baseline modulation depth has not been defined yet for the 131 MHz side band). Although the 131 MHz side band is not foreseen to be used in science mode, it can be interesting for commissioning purposes to select a RoC value that allows some filtering of the 131 MHz. Ideally one should pick up a RoC value that is located at the middle of the interval separating the two local extrema of the purple dotted curve. The nominal RoC has been chosen at 780 mm. This value is almost the optimal one for the filtering of the carrier and the main side bands. In Fig. 6 the yellow-shadowed area indicates the possible location of the RoC value assuming an allowed manufacturing error bar of ± 15 mm centered around the nominal RoC of 780 mm. One can notice that the 131 MHz HOMs are not properly filtered when the OMC RoC is at the margin of the error bars. Therefore, depending on the final error on the RoC value, the 131 MHz side band HOMs may or may not be filtered out by the OMC. One must keep in mind that there is a large uncertainty on the power estimate for the 131 MHz side band. Indeed its factor of merit is limited by the modes of order 9 and 14 and there is not any simulation result available at present time to precisely quantify the amount of power in these modes. In case these high order modes are confirmed to be a problem, one will need to switch off the 131 MHz side band in science mode.

To conclude, a nominal radius of curvature of 780 mm is chosen for each OMC cavity.

4 Advanced Virgo OMC design

Finesse	L_{opt} (mm)	L_{geo} (mm)	RoC (mm)	Waist (μm)	Inc. angle (°)
210 ± 20	178.3 ± 0.6	61.5 ± 0.2	780 ± 15	257.7 ± 1.3	6.00 ± 0.03

Table 1: *Design of the Advanced Virgo OMC cavity with allowed manufacturing error bars. L_{geo} refers to the cavity geometrical length and L_{opt} to the optical length ($L_{opt} = 2nL_{geo}$).*

This section summarizes the refined OMC design. In order to reach sufficient performances in term of side band filtering two OMC cavities are placed in series as shown in the optical drawing in Fig. 3. Motivations for this design have been presented in [3]. The cavities are made of fused silica Suprasil 3001, which guarantees absorption losses equal to or lower than 0.3 ppm/cm. The two cavities are identical. Their geometry is shown on the technical drawing in Fig. 7. The main optical parameters of the OMC cavities are summarized in Tab. 1. The changes with respect to the parameters given in the TDR [3] are the following:

- Each cavity has only one spherical surface, whose nominal radius of curvature is 780 mm.

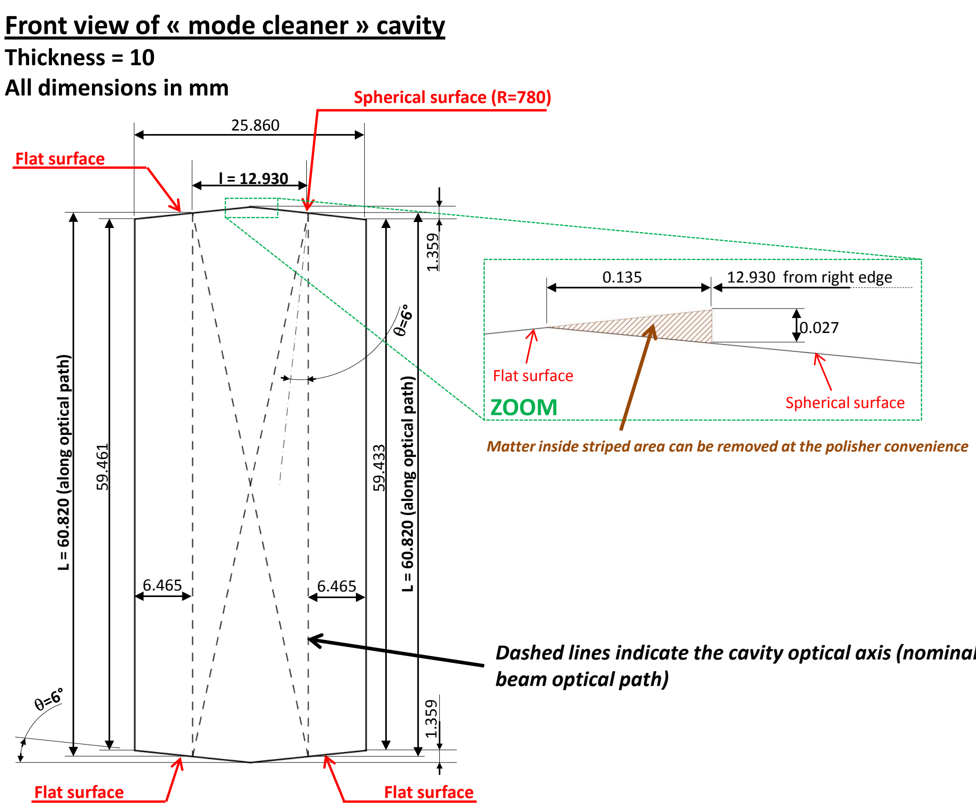

Figure 7: Technical drawing of the mode cleaner cavity. The dimensions are indicated in mm, and the angles in degrees. The piece thickness is 10 mm.

- The nominal angle of incidence of the OMC surfaces has changed from 8.876° to 6.0°. While the new angle should still be sufficiently high to avoid the pick of back-scattering, this choice further reduces the risk of astigmatism (this point will be further discussed in section 7). Moreover it allows to reduce a bit the width of the OMC substrate (from 30 mm to 25.86 mm) which has the advantage to minimize the thermal inertia (which is a relevant point for the thermal control system).

A slightly ammended version of this revised design (with $\rho = 789.2 \pm 3$ mm) might also be considered according to the proposal made by a polishing compagny in a recent offer (see Appendix A).

5 Filtering performances

power recycling 25W			
	$l_{geo} = 61.30$ mm $\rho = 795$ mm	Nominal WP $l_{geo} = 61.50$ mm $\rho = 780$ mm	$l_{geo} = 61.70$ mm $\rho = 765$ mm
Carrier HOM Total	8.2μW	2.0μW	0.8μW
Carrier Specifications	$\leq 75\mu$W		
SB1 TEM_{00}	73μW	72μW	71μW
SB1 HOM	0.3μW	0.06μW	0.02μW
SB1 Total	73μW	72μW	71μW
SB1 Specifications	$\leq 75\mu$W		
SB2 TEM_{00}	0.2 μW		
SB2 HOM	1.2μW	4.1μW	49μW
SB2 Total	1.4μW	4.3μW	49μW
SB2 Specifications	$\leq 75\mu$W		

Table 2: *Transmission of the carrier HOM and side bands after the two OMC cavities in the PR 25W configuration. The transmitted power is computed for three different working points (WP): the nominal WP ($\rho = 780$ mm, $l_{geo} = 61.5$ cm), and two other WPs corresponding to the extrema of the error bars given in Tab. 1. SB1 refers to the side-band at 6.27 MHz and SDB2 to the side-band at 56.44 MHz.*

The transmission factors and the residual powers after the two OMC cavities have been estimated for each mode up to $m + n = 14$ (where m and n refer to the indexes of the TEM modes). Modes of higher order have such an extended spatial profile that they will not be accepted by the system aperture. Concerning the HOM and SB power before the OMC (values of P^N_{car} and P^N_{sb} defined in section 3) the same assumptions have been made as in [3] (see Tab. 7.3

Dual recycling 125W			
	$l_{geo} = 61.30$ mm $\rho = 795$ mm	Nominal WP $l_{geo} = 61.50$ mm $\rho = 780$ mm	$l_{geo} = 61.70$ mm $\rho = 765$ mm
Carrier HOM Total	13.7μW	3.3μW	1.3μW
Carrier Specifications		$\leq 80\mu$W	
SB1 TEM_{00}	21.7μW	21.4μW	21.1μW
SB1 HOM	0.01μW	0.02μW	0.01μW
SB1 Total	21.7μW	21.4μW	21.1μW
SB1 Specifications		≤ 80 μW	
SB2 TEM_{00}		0.3 μW	
SB2 HOM	1.7μW	5.8μW	67.9μW
SB2 Total	1.9μW	6.0μW	68.1μW
SB2 Specifications		≤ 80 μW	

Table 3: *Transmission of the carrier HOM and side bands after the two OMC cavities in the SR 125W configuration. The transmitted power is computed for three different working points (WP): the nominal WP ($\rho = 780$ mm, $l_{geo} = 61.5$ cm), and two other WPs corresponding to the extrema of the error bars given in Tab. 1. SB1 refers to the side-band at 6.27 MHz and SDB2 to the side-band at 56.44 MHz.*

and Tab. 7.4 in the TDR). The residual powers after the OMC cavities have been calculated for three different sets of parameters:

- The nominal set of parameters (or nominal working point) for a geometrical length $L_{geo} = 61.50$ mm and a RoC $\rho = 780$ mm.
- Another set of parameters ($L_{geo} = 61.30$ mm and a RoC $\rho = 795$ mm) has been tested. It corresponds to the worst possible working point in term of transmission of the carrier HOM, when the length and the RoC stay within the error bars given in Tab. 1.
- Another set of parameters ($L_{geo} = 61.70$ cm and a RoC $\rho = 765$ mm) corresponds to the worst possible working point in term of transmission of the HOM of the side band at 56.44 MHz, still according to the error bars given in Tab. 1.

All results concerning the carrier HOM and the side bands (6.27 MHz and 56.44 MHz) TEM_{00} and HOM are summarized in Tab. 2 for the PR 25W configuration and in Tab. 3 for the SR 125W configuration. These tables contain three columns corresponding to the three working points mentioned above. The power expected in the TEM_{00} as well as the sum over all HOM are given. For the side bands the sum between the TEM_{00} and the HOM modes is also provided. These numbers must be compared to the specifications provided by ISC. These specifications are satisfied for the carrier and the two side bands (6.27 MHz and 56.44 MHz).

6 Polishing specifications

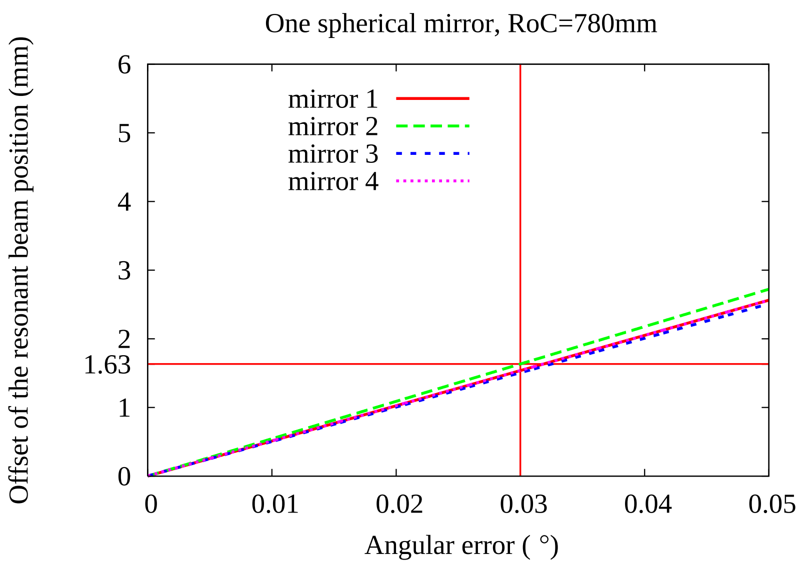

Figure 8: Beam miscentering on the OMC surfaces as a function of the tilt angle error (θ), for the revised OMC design (one spherical surface per cavity and $\rho = 780$ mm).

Cavity length (as measured along the beam optical path between two opposite surfaces)	$L = (60.820 \pm 0.200)\ mm$
Distance between the optical centers of two adjacent surfaces	$l = (12.930 \pm 0.100)\ mm$
Inclination angle of each surface	$\theta = (6.00 \pm 0.03)°$
Radius of curvature of the spherical surface	$R = (780 \pm 15)\ mm$

Table 4: *Main geometrical parameters of the mode cleaner cavity with allowed manufacturing error bars.*

6.1 Geometrical specifications for polisher

Tab. 4 summarizes the main specifications on the OMC geometry to be provided to the polishing company (according to the technical drawing shown in Fig. 7). The length L is directly connected to the cavity geometrical length and the incidence angle θ according to equation 3. The distance between the optical centers of two adjacent surfaces (l) can be derived from L and θ:

$$l = L \times tan(2\theta) \tag{12}$$

As indicated in Tab. 4, errors of ± 15 mm on the radius of curvature and ± 0.2 mm on the main cavity length are accepted. They are compatible with the filtering performances discussed in section 5.
The impact of an error on the cavity surface tilt (θ) has been deeply studied in [4] for the OMC design presented in [3] (made of 2 flat surfaces and two spherical surfaces with $\rho = 1499$ mm). In presence of a static misalignment of the OMC surfaces, the optical axes of the cavity are slightly misaligned and, consequently, the beam is slightly miscentered with respect to the OMC surfaces. The study presented in [4] shows that the maximum miscentering that one can obtain when the maximum angular error is 0.03° corresponds to 1.6 mm. Such miscentering is acceptable as an optical aperture of 4 mm radius is foreseen (see Tab. 5). The study has been repeated for the refined OMC design (single spherical surface per cavity with $\rho = 780$ mm) and the result is shown in Fig. 8. The conclusion is exactly the same.

The manufacturing error bars proposed in Tab. 4 have been accepted by several polishing companies. However one of them is proposing a slight change in the nominal radius of curvature of the spherical surface ($\rho = 789.2$ mm) while guaranteeing a much smaller error bar (± 3 mm). This change would lead to a slightly ammended design, which is discussed in Appendix A.

Diameter of the clear aperture on each surface	8 mm
Surface flatness defects (over the clear aperture of 8 mm)	5 $nm\ RMS$ or $\lambda/40PtV(\lambda = 1064\ nm)$
Micro-roughness (spatial frequencies above 1000 m^{-1}) within clear aperture	$\leq 0.3\ nm\ RMS$ or best effort
No scratch, no digs within clear aperture	

Table 5: *Specifications for the polishing quality of the four mode cleaner reflective surfaces.*

6.2 Specifications on surface quality for polisher

Tab. 5 summarizes the main specifications on the OMC surface quality to be provided to the polishing company.

Although the radius of the beam resonating inside the cavity is lower than 300 μm, a clear aperture of 8 mm diameter centered on each reflective surface is requested in order to allow some error on the surface tilt angle (cf. section 6.1).

The specifications on the surface micro-roughness (≤ 0.3 nm RMS for spatial frequencies above 1000 m^{-1}) and on the surface flatness defects (5 nm RMS over the clear aperture) have been set in order to maintain the total scattering losses below 1%. The choice of these parameters was driven by optical simulations performed with Oscar [8, 9], whose main results are reported in [5]. One can notice that the requirement on the flatness defects should be conservative, as low spatial frequency defects can in principle be compensated when aligning the beam with respect to the OMC cavity. Nevertheless the requested flatness (which correspond to spatial frequencies between 125 and 1000 m^{-1} given the size of the aperture) seems to be consistent with the requested micro-roughness above 1000 m^{-1} and had been accepted by several polishing companies.

7 OMC loss budget

This section gives an overview of the expected OMC losses. First a simple calculation of the expected astigmatism losses is presented. Then the effect of an error on the beam incident angle is discussed. Finally one gives a brief summary of the OMC loss budget.

7.1 Astigmatism losses

Astigmatism losses are induced by two different effects:

- when the beam crosses a tilted vacuum-silica interface;
- when the beam is reflected on a spherical surface with a non-normal incidence.

Crossing of the tilted vacuum-silica interface

When the incident beam enters in the OMC cavity, it crosses a tilted vacuum-silica interface. The situation is schematized in Fig. 9. The diameter of the incident beam (assumed to be perfectly gaussian) is noted A. As shown in Fig. 9 the beam resonating inside the cavity has a larger diameter (noted B) along the horizontal axis of its cross-section. The ratio between the beam dimensions along the horizontal and vertical axes is given by:

$$\frac{B}{A} = \sqrt{\frac{1 - sin^2(\theta)}{1 - n^2 sin^2(\theta)}} \tag{13}$$

This astigmatism induces some mismatching losses given by:

$$Losses = \left(\frac{\Delta w}{w_0}\right)^2 = \left(\sqrt{\frac{1 - sin^2(\theta)}{1 - n^2 sin^2(\theta)}} - 1\right)^2 \tag{14}$$

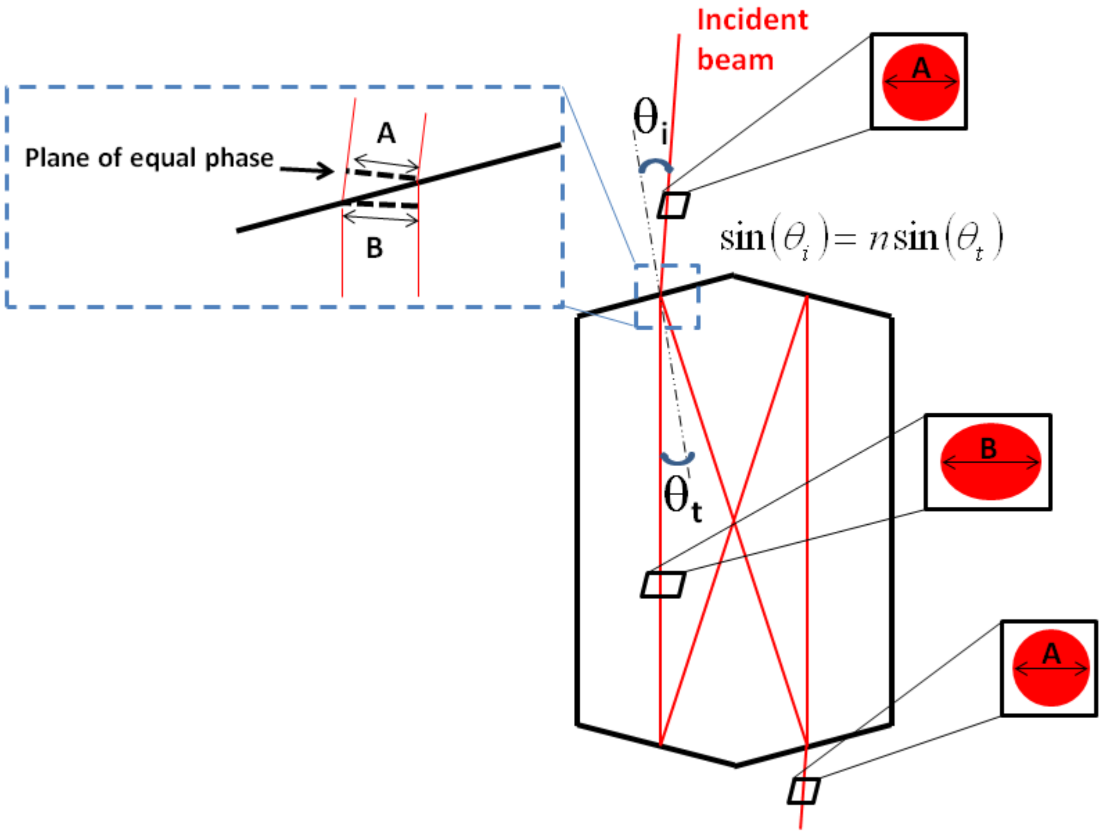

Figure 9: Astigmatism induced by the crossing of the vacuum-silica interface.

With an incident angle of 6°, these losses are equal to 38 ppm.

Reflection on a spherical surface

The beam resonating inside the OMC cavity is reflected on the tilted spherical surface. This induces some astigmatism, which, as shown in [10], is equivalent to a RoC asymmetry along the x and y axes, given by:

$$\Delta\rho \approx \rho\theta^2 \tag{15}$$

This RoC asymetry translates into mismatching losses given by:

$$Losses = \left(\frac{\Delta w}{w_0}\right)^2 \approx \left(\frac{1}{4}\frac{1}{\rho - 2L_{geo}}\rho\theta^2\right)^2 \tag{16}$$

For the OMC design presented in section 4 these losses are equal to 10 ppm.

7.2 Losses induced by angular errors

As explained in *Zomer et al.* [11], misalignments in four mirror cavities can induce gain and polarization instabilities depending on the finesse of the cavity and the number of thin layers composing the reflective coating of the surfaces. Consequently a static error on the surface incidence angle could induce optical losses. This effect also depends on the nominal incidence angle and, according to [11], is not significant for angles lower than 0.1 rad (6°).
Based on the simulation results presented in [11], the maximum losses induced by an error of 500 μrad (0.03°) around a nominal incidence angle of 6°, for a cavity finesse a of few hundred, is expected to be of the order of 0.1%.

7.3 Loss budget summary

The following optical losses are anticipated:

- The internal cavity losses will be dominated by scattering losses, which should be kept lower than 2% for the two cavities according to the polishing specifications provided in Tab. 5.
- As discussed in section 7.1 the losses due to astigmatism are negligible and should be of the order of 100 ppm for the two cavities.
- As discussed in section 7.2, an error on the surface tilt could induce losses of the order of 0.1% due to polarization effects.
- Beam mismatching (related to a mistuning of the mode matching telescope) should induce losses lower than 1% for the two cavities.
- Losses due to misalignment should be of the order of 1.5% (with up to 0.5% losses due to the relative misalignment between the two cavities, and 1% losses due to the beam misalignment).

This budget gives some cavities intrinsic losses of about 2% and misalignment/mismatching losses of about 2.5%.

8 Conclusions

A refined OMC design with a single spherical surface per cavity (and a nominal RoC of 780 mm) has been studied. It satisfies the requirements on the OMC filtering and is proposed as reference design for the polishing specifications.
A design with a slightly modified radius of curvature (789.2 mm) is also presented in Appendix A. This RoC value has been proposed by a polishing company with the benefit of a smaller error bar. This solution also satisfies the requirements and can be used as alternative for the polishing specifications.

References

[1] E. Tournefier, *Advanced Virgo output mode cleaner: specifications*, VIR-0071A-08 (2008).

[2] R. Gouaty, E. Tournefier, B. Mours, P. Mugnier, L. Rolland, *Advanced Virgo output mode cleaner: revision of the specifications*, VIR-0020A-11 (2011).

[3] The Virgo Collaboration, *Avanced Virgo Technical Design Report*, VIR-0128A-12 (2012).

[4] L. Di Gallo, *Maximum allowed angular errors for positioning mirrors in Advanced Virgo OMC*, VIR-0266A-12 (2012).

[5] L. Di Gallo, *Mirror surface studies for Advanced Virgo OMC*, VIR-0267A-12 (2012).

[6] F.J. Raab, S.E. Whitcomb, LIGO-T920004-00-R (1992).

[7] P. Fritschel, LIGO-T060303-00-D (2006).

[8] J. Degallaix, *J. Degallaix, OSCAR a Matlab based optical FFT code*, Journal of Physics Conference Series 228(1):01 2021 (2010).

[9] J. Degallaix, *Oscar, an optical fft code to simulate fabry perot cavities with arbitrary mirror profiles (2012). http://www.mathworks.com/matlabcentral/fileexchange/20607-oscar*

[10] P. Hello, J.Y. Vinet, J. Optics (Paris), vol. 27, 6, pp. 265-276 (1996), VIR-NOT-LAL-1380-96.

[11] F. Zomer, Y.Fedala, N. Pavloff, V. Soskov, A. Variola, *Polarization induced instabilities in external four-mirror Fabry-Perot cavities*, Applied Optics, Vol.48, Issue 35, pp. 6651-6661 (2009).

A OMC design with $\rho = 789.2$ mm

In this appendix a slightly modified OMC design (with respect to section 4) is presented. This alternative design has been studied following a proposal by a polishing company to change the nominal radius of curvature (RoC) to 789.2 mm instead of 780 mm. For this new RoC value the polishing company is able to guarantee a manufacturing error bar of ± 3 mm and to minimize the cost.
The consequence of this modification is that the geometrical length of the OMC cavity must be adjusted in order to minimize the factor of merit (FoM) introduced in section 3 (eq. 11). The optimal geometrical length for a RoC of 789.2 mm is found to be $L_{geo} = 62$ mm. Indeed Fig. 10 shows the evolution of the FoM (sum of the residual carrier HOM and side bands components transmitted by the OMC) as a function of the RoC, with this new assumption on the OMC length. One can see that the total FoM is minimized for a RoC value near 789.2 mm.
The shadowed area in Fig. 10 indicates the possible location of the RoC value, taking into account an allowed manufacturing error bar of ± 3 mm. One can notice that even at the margin of the error bar the total FoM remains close to its minimum. Moreover a good filtering is also obtained for the side band at 131 MHz, which is an asset with respect to the design presented in sections 3 and 4 (see Fig. 6).

Finesse	L_{opt} (mm)	L_{geo} (mm)	RoC (mm)	Waist (μm)	Inc. angle (°)
210 ± 20	179.8 ± 0.6	62.0 ± 0.2	789.2 ± 3	259.0 ± 0.2	6.00 ± 0.03

Table 6: *Design of the Advanced Virgo OMC cavity with allowed manufacturing error bars, for a nominal RoC ρ = 789.2 mm. L_{geo} refers to the cavity geometrical length and L_{opt} to the optical length ($L_{opt} = 2nL_{geo}$).*

Fig. 11 and Tab. 6 summarizes the OMC design obtained after optimizing the geometrical length for the RoC of 789.2 mm. The filtering performances obtained with this design are summarized in Tab. 7 for the PR 25W configuration and in Tab. 8 for the SR 125W configuration. The residual power obtained in transmission of the OMC has been evaluated using the same assumptions on the HOM and SB power before the OMC as it is done in [3] (see Tab. 7.3 and Tab. 7.4 in the TDR).
In Tab. 7 and Tab. 8 the residual power in the carrier HOM and in the side bands components obtained in transmission of the OMC cavities is shown for 3 different working points:

- The nominal set of parameters (or nominal working point) for a geometrical length $L_{geo} = 62$ mm and a RoC $\rho = 789.2$ mm.
- Another set of parameters ($L_{geo} = 61.80$ mm and a RoC $\rho = 792.2$ mm) has been tested. It corresponds to the worst possible working point in term of transmission of the carrier HOM, when the length and the RoC stay within the error bars given in Tab. 6.

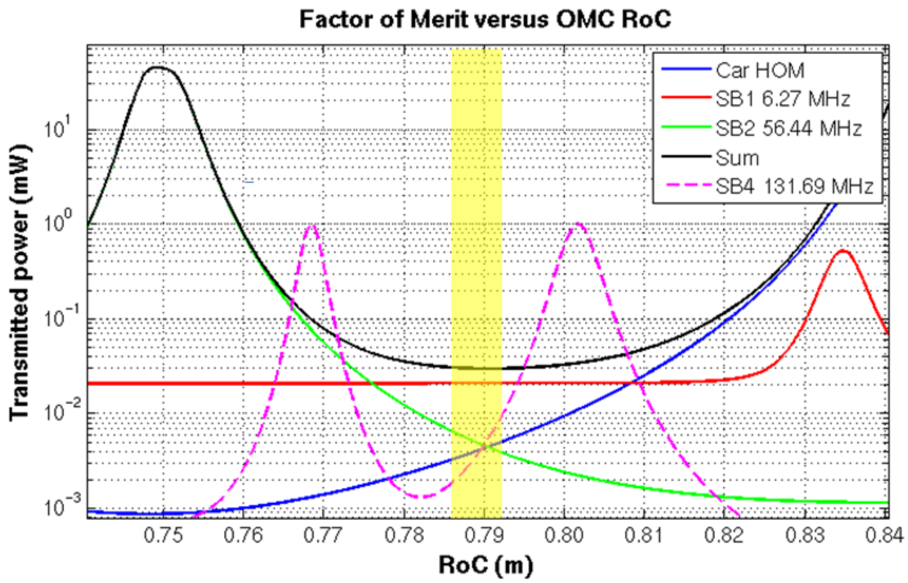

Figure 10: Sum of side bands and high order modes in transmission of the OMC (B1 beam) as a function of the OMC RoC, for a nominal geometrical length $L_{geo} = 62$ mm. The black curve stands for the total factor of merit (FoM) that includes the sum of all carrier higher order modes, and all 6.27 MHz and 56.44 MHz side band components. The blue curve corresponds to the carrier FoM (sum of carrier HOMs). The red curve (respectively green) stands for the contribution of the 6.27 MHz (respectively 56.44 MHz) side band. A FoM has also been calculated for the 131 MHz side band and is shown as the purple dotted curve. The yellow shadowed area represents the possible location of the RoC, assuming a nominal value of 789.2 mm with an allowed error bar of ± 3 mm.

- Another set of parameters ($L_{geo} = 62.20$ cm and a RoC $\rho = 786.2$ mm) corresponds to the worst possible working point in term of transmission of the HOM of the side band at 56.44 MHz, still according to the error bars given in Tab. 6.

Tab. 7 and Tab. 8 show that the filtering performances of the OMC cavities match the requirements. Furthermore the performances at the margin of the error bars are improved with respect to Tab. 2 and Tab. 3 due to the more constrained RoC error bar proposed by the polishing company.

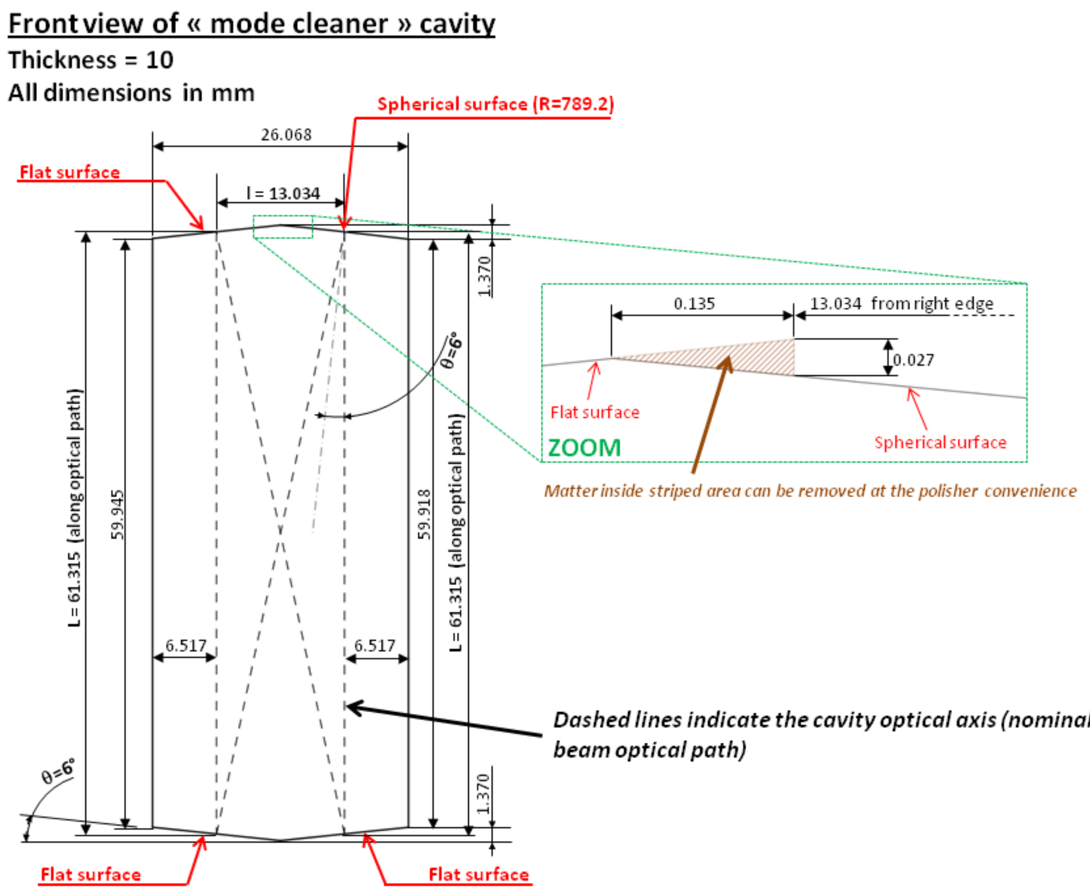

Figure 11: Technical drawing of the mode cleaner cavity with $\rho = 789.2$ mm. The dimensions are indicated in mm, and the angles in degrees. The piece thickness is 10 mm.

power recycling 25W			
		Nominal WP	
	$l_{geo} = 61.80$ mm $\rho = 792.2$ mm	$l_{geo} = 62.00$ mm $\rho = 789.2$ mm	$l_{geo} = 62.20$ mm $\rho = 786.2$ mm
Carrier HOM Total	3.7μW	2.4μW	1.7μW
Carrier Specifications	$\leq 75\mu$W		
SB1 TEM_{00}	71μW	70μW	69μW
SB1 HOM	0.12μW	0.08μW	0.05μW
SB1 Total	71μW	70μW	69μW
SB1 Specifications	$\leq 75\mu$W		
SB2 TEM_{00}	0.2 μW		
SB2 HOM	2.1μW	3.3μW	5.8μW
SB2 Total	2.3μW	3.5μW	6.0μW
SB2 Specifications	$\leq 75\mu$W		

Table 7: *Transmission of the carrier HOM and side bands after the two OMC cavities in the PR 25W configuration. The transmitted power is computed for three different working points (WP): the nominal WP (ρ = 789.2 mm, l_{geo} = 62.0 cm), and two other WPs corresponding to the extrema of the error bars given in Tab. 6. SB1 refers to the side-band at 6.27 MHz and SDB2 to the side-band at 56.44 MHz.*

Dual recycling 125W			
	$l_{geo} = 61.80$ mm $\rho = 792.2$ mm	Nominal WP $l_{geo} = 62.00$ mm $\rho = 789.2$ mm	$l_{geo} = 62.20$ mm $\rho = 786.2$ mm
Carrier HOM Total	6.1μW	4.1μW	2.8μW
Carrier Specifications		$\leq 80\mu$W	
SB1 TEM_{00}	21.0μW	20.8μW	20.5μW
SB1 HOM	0.04μW	0.02μW	0.02μW
SB1 Total	21.0μW	20.8μW	20.5μW
SB1 Specifications		≤ 80 μW	
SB2 TEM_{00}		0.3 μW	
SB2 HOM	3.0μW	4.6μW	8.0μW
SB2 Total	3.2μW	4.9μW	8.3μW
SB2 Specifications		≤ 80 μW	

Table 8: *Transmission of the carrier HOM and side bands after the two OMC cavities in the SR 125W configuration. The transmitted power is computed for three different working points (WP): the nominal WP (ρ = 789.2 mm, l_{geo} = 62.0 cm), and two other WPs corresponding to the extrema of the error bars given in Tab. 6. SB1 refers to the side-band at 6.27 MHz and SDB2 to the side-band at 56.44 MHz.*